Science of the Total Environment 954 (2024) 176619

Contents lists available at ScienceDirect

Science of the Total Environment

journal homepage: www.elsevier.com/locate/scitotenv

Decadal changes in microplastic accumulation in freshwater sediments: Evaluating influencing factors

Jutamas Bussarakum [a], William D. Burgos [a], Samuel B. Cohen [b,c], Kimberly Van Meter [b,c], Jon N. Sweetman [d], Patrick J. Drohan [d], Raymond G. Najjar [e], Jill M. Arriola [e], Katharina Pankratz [a], Lisa A. Emili [f], Nathaniel R. Warner [a,*]

[a] Department of Civil and Environmental Engineering, The Pennsylvania State University, University Park, PA 16802, USA
[b] Department of Geography, The Pennsylvania State University, University Park, PA 16802, USA
[c] Earth and Environmental Systems Institute, The Pennsylvania State University, University Park, PA 16802, USA
[d] Department of Ecosystem Science and Management, The Pennsylvania State University, University Park, PA 16802, USA
[e] Department of Meteorology and Atmospheric Science, The Pennsylvania State University, University Park, PA 16802, USA
[f] Department of Earth and Mineral Sciences, Penn State Altoona, The Pennsylvania State University, Altoona, PA 16601, USA

HIGHLIGHTS

- MP abundance and dominant morphology varied among 4 age-dated sediment cores.
- No correlation between MP abundance and urban area or population in watersheds
- Open water area within a watershed correlated with MP abundance.
- MP abundance in sediment increased with plastic production from 1950s–2010s.

GRAPHICAL ABSTRACT

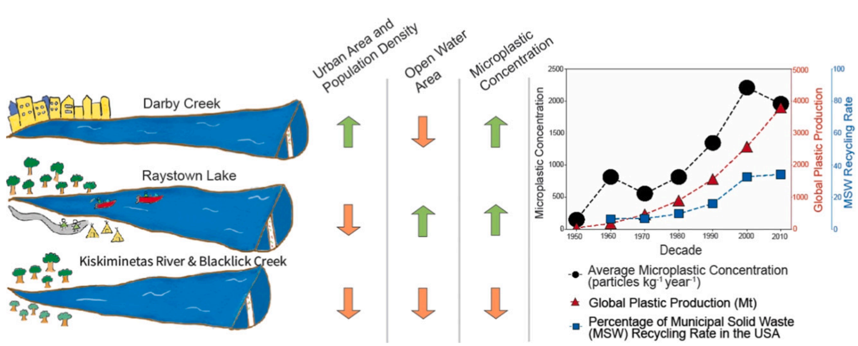

ARTICLE INFO

Editor: Jay Gan

Keywords:
Microplastics
Plastic pollution
Sediment
Age dating
Urban area
Population density

ABSTRACT

Microplastics are small plastic particles with sizes ranging between 1 μm and 5 mm. Microplastics can originate from macro plastics and degrade to a smaller size or be produced directly by manufacturers. Few studies have examined microplastic contamination in freshwater sediment cores to estimate changes in microplastic contamination over time. We present the results of a study that examined sediment cores from four watersheds, Kiskiminetas River, Blacklick Creek, Raystown Lake, and Darby Creek, in Pennsylvania, USA to reveal the history of microplastic accumulation and factors that contribute to microplastic distribution. The abundance and morphology of microplastics varied over time and between these four locations. The highest microplastic abundance was found in Raystown Lake, ranging from 704 to 5397 particles kg^{-1} with fiber as the dominant microplastic type, while Darby Creek (0–3000 particles kg^{-1}), Kiskiminetas River (0–448 particles kg^{-1}), and Blacklick Creek (0–156 particles kg^{-1}) had lower microplastic concentration. Moreover, Darby Creek had the most diverse microplastic morphology and a trend of decreasing concentration with depth. Although the Darby

* Corresponding author.
E-mail address: nrw6@psu.edu (N.R. Warner).

https://doi.org/10.1016/j.scitotenv.2024.176619
Received 16 May 2024; Received in revised form 20 September 2024; Accepted 28 September 2024
Available online 1 October 2024

Creek watershed has the most developed area and highest population density, it did not have the highest microplastic concentration. Averaged over the four cores, microplastic abundance increased as global plastics production increased from the 1950s–2010s. Our findings provide insights into the fate and transport of microplastic contamination in freshwater environments, which is vital to establishing sustainable mitigation strategies.

1. Introduction

Plastic pollution is a global environmental threat. Due to beneficial properties including durability, flexibility, and low cost, global plastic production has increased exponentially from 2 million metric tons (Mt) produced in 1950 to 391 Mt. by 2021 (Europe, 2022; Jambeck and Walker-Franklin, 2023; Wickham et al., 2021). Approximately, 90 % of plastic is derived from fossil fuels (Europe, 2022). Single-use plastics (36 %) and synthetic textiles (14 %) make up 50 % of plastic production and are the main contributors to plastic pollution (Geyer et al., 2017; Xia Zhu, 2021). More than half of plastic waste ends up in landfills; only one-tenth is recycled, and >80 % of mismanaged waste is estimated to be transported by rivers to coastal environments (Geyer et al., 2017; Peng et al., 2020).

Plastics in the environment degrade to highly persistent microparticles, commonly known as microplastics (J. P. G. L. Frias and Nash, 2019; Hanif et al., 2022). Microplastics (MPs) are defined as polymer-based structures or synthetic solid particles, that are water-insoluble and vary in size from 1 μm to 5 mm (Frias and Nash, 2019). These MPs may be primary, originating through direct release from industrial processes, or secondary, forming from the biological, thermal, and photolytic degradation of larger plastic particles (Andrady, 2011; Frias and Nash, 2019). Microplastic contamination has been reported in water, sediment, air, plants, and food; leading to MP uptake by living organisms and humans (Baldwin et al., 2020; Leslie et al., 2022; Yue Li et al., 2023; Senathirajah et al., 2021). This contamination has become a concern to the public because of the potential adverse effects on human health and aquatic life (Felipe-Rodríguez et al., 2022). As a consequence, the United Nations Sustainable Development Goals emphasized the need for action to reduce MP pollution under Goal 14: Life Below Water (Walker, 2021). The rationale for concern is that MP ingestion by animals potentially causes metabolic disorders, immunotoxicity, neurotoxicity, and developmental toxicity (Kannan and Vimalkumar, 2021). However, there remains uncertainty about the concentration of MPs that can cause adverse effects on living organisms because of variability in MP types, including chemical composition, size, and morphology, as well as limited data available to quantify dose-response relationships and exposure (Yue Li et al., 2023).

A myriad of factors control the transport and fate of MPs in the aquatic environment (Mendrik et al., 2023). Understanding the interplay of these factors is an emerging area of research (Moyal et al., 2023). Microplastic buoyancy, and conversely settling, is dependent on the physical-chemical properties of MPs such as size, shape, density, and chemical composition. As MPs move through aquatic environments they undergo degradation by ultraviolet radiation, chemical oxidation, microbial decomposition, and mechanical means (Lin et al., 2022). Degradation alters the size, density, and surface chemistry of individual MP particles (Lin et al., 2022; Moyal et al., 2023). Further, the settling of MP particles is impacted by the aggregation of particles and the formation of biofilms (Jiang et al., 2021; Pete et al., 2023). These factors make it challenging to predict MP contamination in sediment, as it is not always straightforward to detect only high-density MPs in both freshwater and marine sediments (Rogers et al., 2020). Moreover, few studies have examined the long-term accumulation of MPs in sediments, which limits our ability to assess changes in MP accumulation rates, concentrations, or the overall function of sediment as a sink for MPs (Osorio et al., 2021; Yuan et al., 2023). Yet, sediment cores collected from depositional areas have long been used to reveal historical changes in watersheds and aquatic environments that may have been induced by changes in hydrology, human activities, or land use (B. Li et al., 2022; Smol, 2019). By analyzing MPs in dated sediment cores, rates of MP deposition and burial can be calculated over longer periods (Dong et al., 2020; Turner et al., 2019).

To date, most MP studies have focused on marine environments with considerably less attention on freshwater systems (D'Avignon et al., 2021). Our understanding of historical contamination, potential transport of MPs within sediment, and factors contributing to MP burial in freshwater sediment remains limited. Despite the lack of attention, researchers have found freshwater streams can accumulate MPs sourced from terrestrial human activities (B. Li et al., 2022), flooding events (Culligan et al., 2021), and atmospheric deposition (Villanova-Solano et al., 2023) and then transport MPs to the ultimate sink, the marine environment. Correlative relationships between MP concentrations and urban development, such as population and gross domestic product, have been previously observed but focused on modern surficial sediment collected from a single watershed (B. Li et al., 2022; Yuan et al., 2023). In the United States of America (USA), few studies have reported MP concentrations in freshwater sediment cores, which emphasizes the limited data available to comprehend changes in MP contamination over time (Baldwin et al., 2020; Culligan et al., 2021).

This study focused on the temporal distribution of MP abundance in sediments of four watersheds in Pennsylvania (PA), USA. We hypothesize that freshwater sediment 1) accumulates MPs, 2) serves as a record of historical plastic use within a local watershed, and 3) MP accumulation varies based on human activities within the watershed. To test these hypotheses we: a) evaluated changes in MP abundance, morphology, size, and color variation over time within freshwater sediment cores collected from multiple watersheds; b) examined the role of sediment as a MP sink; c) determined if land cover, human activity, and urban development within a watershed are reflected in MP accumulation over historical time; and d) studied the potential of sedimentary factors, including sedimentation rate and organic matter content to influence MP abundance in sediment cores.

2. Material and methods

2.1. Study sites

Sample locations were chosen to represent 1) a range of watershed sizes from >4500 km^2 to <250 km^2, 2) a range of land use (>80 % to <10 % urban) and population densities, and 3) sediment accumulation areas to provide a time series of "pre-plastic" (if possible) through to present day sediment deposition. To represent the above conditions, sediment cores were collected from four locations with persistent depositional patterns and coherent sedimentation records to reduce the chance of sediment scour: Kiskiminetas River, Blacklick Creek, Raystown Lake, and Darby Creek, PA, USA where the water level is maintained by Lock #4, Conemaugh Dam, Raystown Dam, and sea level, respectively (Fig. 1).

The largest catchment area is represented by the Kiskiminetas River, which is located downstream of Blacklick Creek and flows into the Allegheny River (Fig. 2A). This area features a water trail called the Kiski-Conemaugh River Water Trail, suitable for canoeing and kayaking with water level control by Lock #4 on the Allegheny River (Allegheny Ridge Corporation, 2023). One core was collected 1 m from the bank during the summer of 2018 with a Russian-style peat corer. Blacklick

Creek is the largest area based on hydrologic unit code (HUC) 12 and is located between Cambria and Indiana Counties in western PA and drains into the Conemaugh River Lake created by damming the Conemaugh River (Fig. 2B). Depositional modeling, age-dating, and trace metal concentrations within the core were reported previously (Burgos et al., 2017). Raystown Lake is a part of the Lower Raystown Branch of the Juniata River watershed. Raystown Lake is a reservoir created by damming the Juniata River in Huntingdon County and is a popular recreation area for camping, boating, swimming, fishing, and hiking. Three cores were collected from different locations in Raystown Lake (Fig. S1) for radiometric dating. Only one core, selected from the middle of the reservoir and situated downstream from the Seven Points recreational site in Raystown Lake, represented a long-term accumulation of depositional sediment (Fig. 2C). Darby Creek is the smallest watershed studied and meanders through an urbanized area before draining to a tidal marsh that is part of the John Heinz National Wildlife Refuge at Tinicum, Philadelphia, before joining the Delaware River. Two cores were collected in this location (Fig. S2). Only one sediment core collected in the tidal marsh adjacent to the main channel of Darby Creek roughly in the middle of the refuge showed long-term sediment deposition (Fig. 2D).

Sampling methods varied among the four watersheds due to differences in water depths, environmental conditions, boat access and the convenience of using certain tools, (Glew et al., 2001; Skilbeck et al., 2017; Yuan et al., 2023). The details of core sampling are provided in Table 1. All sediment samples were stored at 4 °C until analysis.

2.2. Sediment age model

Sediment chronologies were analyzed using the natural decay of lead-210 (^{210}Pb), which has two sources in sediment. Supported ^{210}Pb, originates from the decay of radium-226 (^{226}Ra) within the sediment and will be in secular equilibrium with parent isotopes (e.g., radium, radon). In contrast, excess ^{210}Pb falls from the atmosphere onto the ground surface and is captured by sediment. This ^{210}Pb is in excess to that supported by radium and begins to decay. The concentration will be highest at the surface and decrease over time according to the law of radioactive decay (Baud et al., 2022).

For all sites, sediment cores were sectioned into 1 cm intervals and then dried in the oven at 60 °C for 24 h. Dried sediment was transferred to a 5 cm petri dish, weighed, sealed with hot glue, and incubated for a minimum of 3 weeks. Resulting dry sediment typically weighed 10 g and was packed in petri dishes to maintain consistent geometry. ^{210}Pb, ^{226}Ra, and cesium-137 (^{137}Cs) activities were measured on the 1 cm intervals using a Mirion Broad Energy Germanium detector. Total count times were between 48 and 72 h. The activity of ^{210}Pb was determined by gamma emission at 46.5 keV and ^{226}Ra was determined by the average of daughter products of ^{214}Pb at 295 and 351 keV, and ^{214}Bi at 609 keV. ^{137}Cs activities were measured at 661 keV and used to validate the age model since ^{137}Cs is not mobile in freshwater sediment environments, indicating a reliable chronology validator (Wang et al., 2022). ^{137}Cs was introduced into the environment by nuclear testing starting in 1952, and the activity peak in 1963 corresponds to the last atmospheric nuclear test before the 1964 moratorium (Ma et al., 2013). Data are reported as Bq kg^{-1} of dry sediment weight.

The ^{210}Pb-based age exploited the 22-year half-life of this isotope and was calculated either using the Constant Initial Concentration (CIC) model or the Constant Rate of Supply (CRS) model, depending on excess ^{210}Pb profiles in sediment cores. These models are, respectively:

$$t = \frac{1}{\lambda} ln \frac{C_0}{C_i} \tag{1}$$

$$t = \frac{1}{\lambda} ln \frac{A_0}{A_i} \tag{2}$$

where t is the sediment deposition age (year), λ is the radioactive decay constant of ^{210}Pb (0.0312 yr^{-1}), C_0 is the concentration of excess ^{210}Pb at the surface, C_i is the concentration of excess ^{210}Pb (calculated by subtracting the ^{226}Ra concentration from the total ^{210}Pb concentration) at any depth of i, A_0 is the total concentration of excess ^{210}Pb in the sediment core, and A_i is the total concentration of excess ^{210}Pb below the depth of i (Baud et al., 2022; De Souza et al., 2012). The CIC model was applied when the excess ^{210}Pb concentration was introduced into the sediment at a constant flow rate and that sedimentation rate remained constant (Sanchez-Cabeza and Ruiz-Fernández, 2012). Under these conditions, the excess ^{210}Pb concentration remained constant within sediment layers. The CRS model was used when the flux of excess ^{210}Pb to the sediment surface was constant, but the sedimentation rate may change. This could lead to a decrease in excess ^{210}Pb as sediment accumulated (De Souza et al., 2012).

2.3. Organic matter analysis

Two to four grams of dry sediment sample was placed into a crucible and heated to 550 °C for 2 h in a muffle furnace (Heiri et al., 2001). After the sample cooled, the weight of the ash sample was recorded, and the percentage of organic matter was calculated using:

$$\%\text{Organic Matter} = \frac{[(Dry\ Weight - Ash\ Weight) \times 100]}{Dry\ Weight} \tag{3}$$

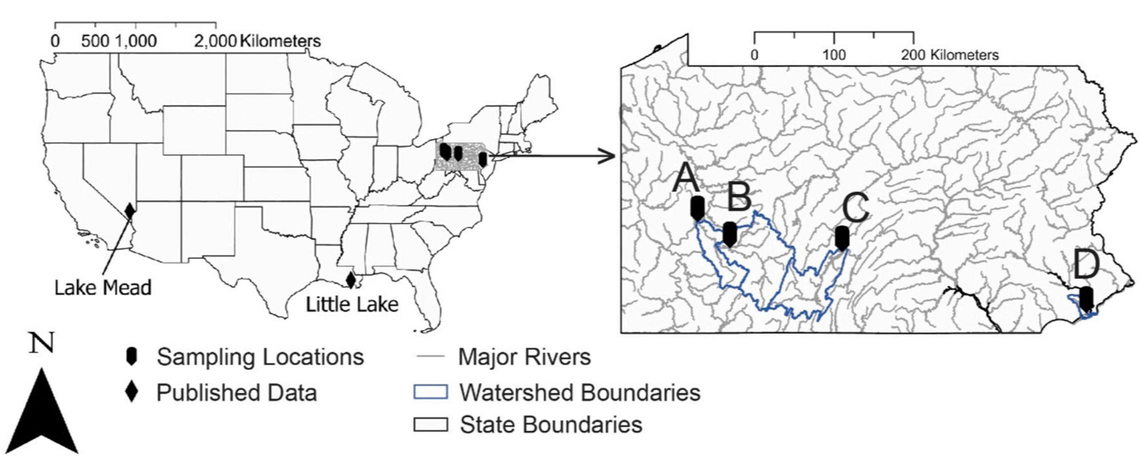

Fig. 1. Locations of sediment cores used in this study. Four watersheds were sampled: Kiskiminetas River (A), Blacklick Creek (B), Raystown Lake (C), and Darby Creek (D) in Pennsylvania. Published data from sediment cores from two locations, Lake Mead in Nevada and Little Lake in Louisiana were sourced from published papers (Baldwin et al., 2020; Culligan et al., 2021, respectively).

2.4. Microplastic extraction

Dry sediment samples (ranging from 4 to 20 g) were added to 30 mL of 10 % H_2O_2 (Frias et al., 2018). Samples were stirred with a stainless-steel spatula for 1 min. Samples were left at room temperature for 10 min before incubation for 5 h at 40 °C and then at room temperature overnight. For density separation, sodium chloride (NaCl) was used in this study because it is environmentally friendly and low-cost. This approach may underestimate high-density MPs such as PVC, which has a low extraction efficiency of 37 % (Duong et al., 2022). However, PVC has not been commonly found in freshwater sediment (Koutnik et al., 2021). 200 mL of saturated NaCl solution (0.35 g mL^{-1}) was added to samples and mixed with a stainless-steel spatula for 1 min (Kazmiruk et al., 2018). After the sediment had settled, the supernatant solution was decanted into a 45 μm sieve and collected in a stainless-steel bowl. The NaCl solution was transferred from the bowl back into the beaker, repeating the density separation two more times. All retained particles on the sieve were collected in a new beaker with Milli-Q® water. Then, 500 μL of 30 % H_2O_2 was added to the sample (~20 mL) until the final concentration of the solution reached 0.73 % for post-organic matter removal. Samples were then incubated overnight at room temperature (Xiaopeng Zhu et al., 2021). Both sample and NaCl solutions were filtered through a 0.45 μm filter (47 mm Ø, GN-6 Metricel® Grid, Pall Corporation) (Ben-David et al., 2021). Milli-Q® water was used to rinse the beaker and the edges of the filter apparatus to obtain any remaining MPs. The filter was then stored in a 5-cm plastic petri dish with the cap

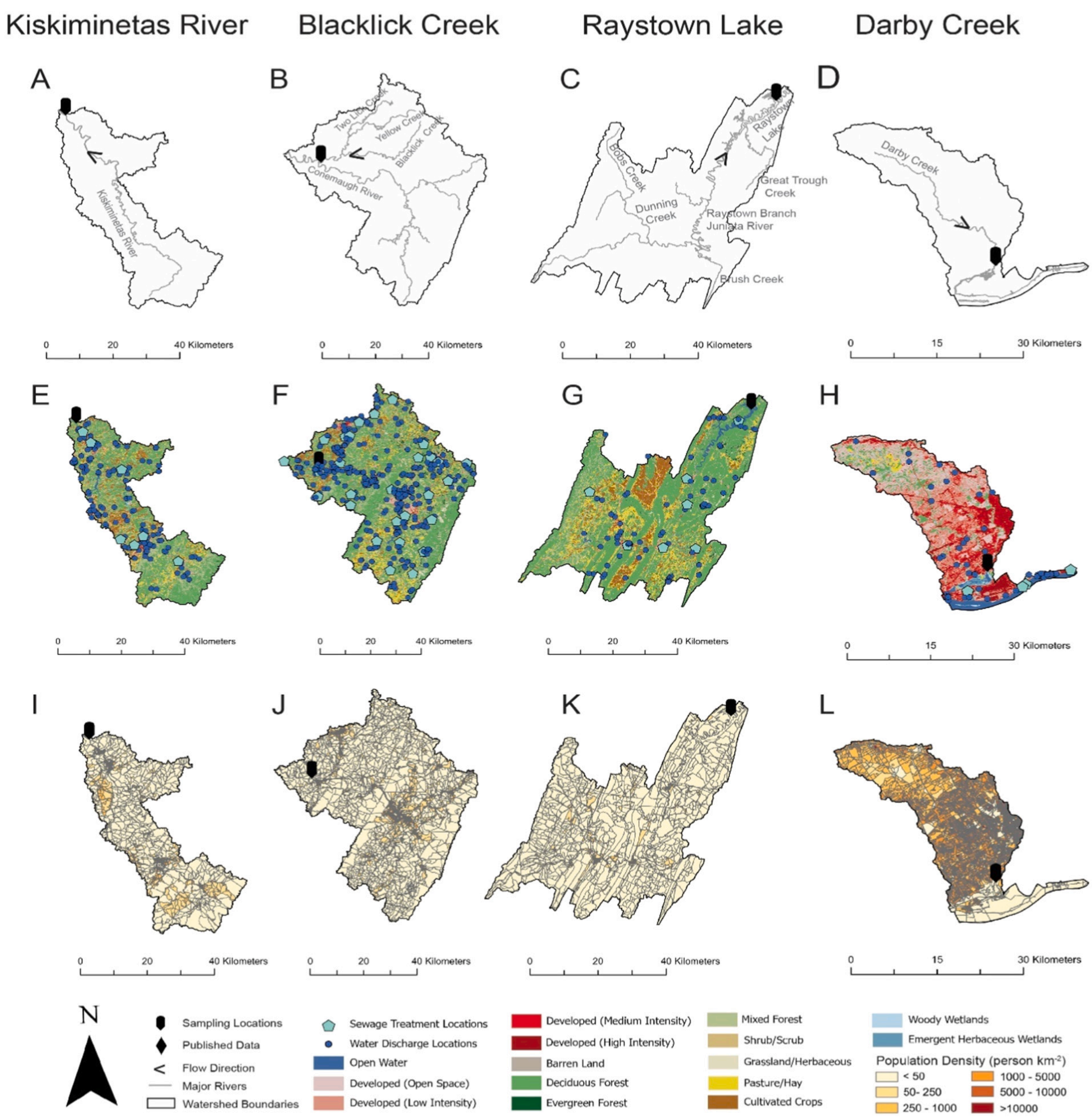

Fig. 2. Site characterization in Kiskiminetas River (A, E, I), Blacklick Creek (B, F, J), Raystown Lake (C, G, K), and Darby Creek (D, H, L) presented for each hydrological unit code (HUC)-8. The top panels (A-D) showed the watershed size and major rivers in each watershed. The middle panels (*E*-H) present land cover categorized by types including Open Water, Developed, Barren, Forest, Shrub/Scrub, Grassland/Herbaceous, Planted/Cultivated, and Wetlands based on NLCD 2021, USGS. The blue circles represent permitted water discharge locations for mineral, industrial, and commercial activities. The light blue pentagonal symbols denote sewage water discharge locations. The bottom panels (I-L) show population density (persons km^{-2}) calculated based on census blocks, which are boundaries defined by visible and identifiable features such as roads, streams, railroads, and townships.

Table 1
Study locations.

Locations	Sampling sites			
	Kiskiminetas River	Blacklick Creek	Raystown Lake	Darby Creek
Coordinates				
Latitude	40.673385	40.44999	40.416944	39.885001
Longitude	−79.65474	−79.29025	−78.020278	−75.264494
HUC size (km^2)	1335	3555	2492	225
Catchment area (km^2)	4889	1084	2455	167
Distance from shore (m)	1	5	240	172 (high tide)
Depth of sediment core (cm)	134	135	80	101
Core sampling method	Peat sampler	Vibracore	ARI Universal Percussion Corer	Peat sampler
Sampling date	June 2018	May 2015	June 2022	September 2022

slightly open and placed in a desiccator at room temperature until dry.

Filters were examined under a stereomicroscope (magnification ranging from 50× to 150×) where color and morphology of MPs were recorded. Suspected plastic particles were tested with the hot tip of a thin needle, resulting in either melting or curling if they were plastic particles (De Witte et al., 2014). The size of MPs was measured by AmScope software version 4.11.21973.20230107. The minimum detectable size for visual analysis in this study was 35 μm, while the software calibration allowed the detection of sizes down to 10 μm. The morphological shapes were classified into four categories: pellets (hard or rounded shape), fibers (rod or fibrous shape), fragments (hard or jagged shape), and films (thin plane of flimsy shape) (Free et al., 2014).

2.5. Quality control and recovery test

MPs are ubiquitous in the environment. To reduce the potential for contamination to the greatest extent possible we conducted several quality control measures. First, all reagent solutions and Milli-Q® water used in the experiment were filtered with a 0.45 μm filter. Glassware was cleaned with 1 % Alconox and rinsed three times with filtered Milli-Q® water, covered with foil, and allowed to dry in the oven at 90 °C. During the extraction process, all beakers were covered with aluminum foil. All processes were conducted in the fume hood, except for the incubation process at 40 °C. A cotton lab coat was always worn.

Ten milliliters of Milli-Q® water was processed as a method blank sample and underwent the same procedures as extracted samples to determine if the materials and laboratory contained notable MPs. These method blank counts of MPs, ranging from 8 to 16 pieces of fiber MPs in the blank samples, were deducted from all samples for accurate microplastic abundance. An MP recovery test was also conducted where sediment was spiked with 6 pieces of microplastic, each approximately 1–5 mm in size, including 3 pieces from plastic bags (High-density polyethylene; HDPE) and 3 pieces from a plastic cup (Polystyrene; PS). The MP extraction was performed on this recovery sample using the procedures noted above. Finally, we examined the morphology and color of all samples for potential piston sample corer contamination from either the plastic caps (orange fragments) or the polycarbonate core sleeve (clear fragments). Neither orange nor clear fragments were observed in the piston corer sample (Raystown Lake).

2.6. Land cover

Land cover data from 2001 to 2021 were downloaded from the National Land Cover Database (NLCD) of the United States Geological Survey (USGS). Land cover was mainly classified into eight categories, including Open Water, Developed, Barren, Forest, Shrub/Scrub, Grassland/Herbaceous, Planted/Cultivated, and Wetlands (Wickham et al., 2021). Population information was collected in 2020 by the U.S. Census Bureau and population density (person km^{-2}) was calculated by the boundaries defined by census blocks, which indicated visible and identifiable features such as roads, streams, railroads, and townships. The streams, trails, watershed boundaries, and water discharges within the watershed were collected from the Pennsylvania Spatial Data Access (PASDA) and the National Pollutant Discharge Elimination System (NPDES) (Pennsylvania Department of Environmental Protection, 2023a). All spatial mapping was conducted using ArcGIS Pro 3.1.1. A Generalized Linear Regression (GLR) model was developed to explore the relationships between MPs in sediment cores and explanatory variables. Explanatory values, such as catchment size, distance to sewage treatment, population density, and land use were extracted within watershed boundaries at each sample location. Each core sediment MP value was treated separately while assigning the same explanatory variables to each location assuming the variable does not change over the core time span based on our review of available changes in the 20 years, 2000 to 2020 and authors historical knowledge of the areas. GLR analysis was conducted using the Spatial Statistics tools available in ArcGIS Pro 3.2.2. The GLR model was formulated as follows:

$$Y = \beta_0 + \beta_1 X_1 + \beta_2 X_2 + \ldots + \beta_n X_n + \varepsilon.$$

Where:Y represents the response variable (MPs in sediment).β_0 represents the intercept term.β_1, β_2, …, β_n represents the coefficients for each explanatory variable X_1, X_2, …, X_n.ε represents the error term.

Model selection and subsequent explanatory variables were selected using parameter variance inflation factors, *p*-value significance, and Akaike Information Criterion (AIC) values. Model fit was assessed using the coefficient of determination (R^2).

2.7. Microplastics comparison data

For comparison, we obtained published data on MPs in sediment from freshwater and brackish environments. Previously published data presented here were searched from the Web of Science database with the keywords “Sediment Core”, “Freshwater”, and “Microplastics” in April 2023. There were 18 results of research articles, but only two provided sedimentation rates with MP concentrations in the USA (Fig. 1): (1) Baldwin et al. (2020), a study of Lake Mead, Nevada, a reservoir along the Colorado River and (2) Culligan et al. (2021), a study of Little Lake, Louisiana, a microtidal brackish lake.

2.8. Statistical analysis

The data for MP concentrations and sedimentation rate were transformed to a log scale and analyzed with the Shapiro-Wilk test for normality, Pearson's Correlation analysis, and Spearman's Rank-Order Correlation. The significance level was set at an alpha of 0.05 and statistical analysis was performed using R version 4.2.3.

3. Results

3.1. Land use

Human activities were examined, including land use, land use change, permitted discharges, population density, and recreation activities in each watershed. Land cover distributions varied among the four locations (Fig. 2 *E*–H). In the Kiskiminetas River watershed, 64 % of the land cover was Forest, followed by 19.6 % with Plant/Cultivated areas and 14 % with Developed areas. Similarly, almost 70 % of the land cover in Blacklick Creek was classified as Forest and Plant/Cultivated areas. Raystown Lake was mostly covered by Forest and Plant/Cultivated (90 %). At hydrological unit code (HUC) 12, Raystown Lake was covered with Open Water areas up to 17 %, while the other locations presented <2 % Open Water areas. Darby Creek had the highest percentage of developed land (>80 %).

Along with developed land cover, the Darby Creek watershed also had the highest population density (2200 persons km^{-2}) (Fig. 2 I–L). In contrast, Kiskiminetas River, Blacklick Creek, and Raystown Lake had much lower population densities of 142, 62, and 20 persons km^{-2}, respectively. Despite a low population, Raystown Lake has more recreational areas, specifically trails, with 568 km compared to Blacklick Creek with 493 km, Kiskiminetas River with 197 km, and Darby Creek with 32 km (Fig. S5).

Each watershed had a variety of point source discharges based on data published in 2023 from the Water Use Planning Program (Pennsylvania Department of Environmental Protection, 2023c), Water Pollution Control Program (Pennsylvania Department of Environmental Protection, 2023b), and NPDES permitting (Pennsylvania Department of Environmental Protection, 2023a). Blacklick Creek showed the highest number of discharge points from industrial use, commercial use, and mineral use, while Raystown Lake had the least. Regarding the number of sewage treatment points, there were 30 in Blacklick Creek, 7 in Kiskiminetas River, 7 in Raystown Lake, and 0 upstream in Darby Creek.

3.2. Sediment core chronologies

Based on radiogenic profiles of ^{210}Pb and ^{137}Cs all four sediment core locations (Fig. 3 A–D) appear to have remained undisturbed and were not eroded or mixed by large hydrological events. The sediment core at Kiskiminetas River (134 cm) showed a long deposition before 1952 based on ^{137}Cs data which showed the absence of ^{137}Cs below a depth of 102 cm (Fig. 3A). The sediment core at Blacklick Creek was the longest collected in this study (135 cm) but only revealed a sediment profile from roughly 1990 to the present (Burgos et al., 2017) (Fig. 3B). The cores in Raystown Lake and Darby Creek represent a much longer sedimentation record. Raystown excess ^{210}Pb concentration was not found below a depth of 40 cm and the peak of ^{137}Cs concentration was observed at a depth of 30 cm, corresponding to the year 1963. Likewise, ^{137}Cs was not observed at a depth of 45–80 cm, indicating sediment deeper than 45 cm was deposited prior to 1952 (Fig. 3C). Darby Creek

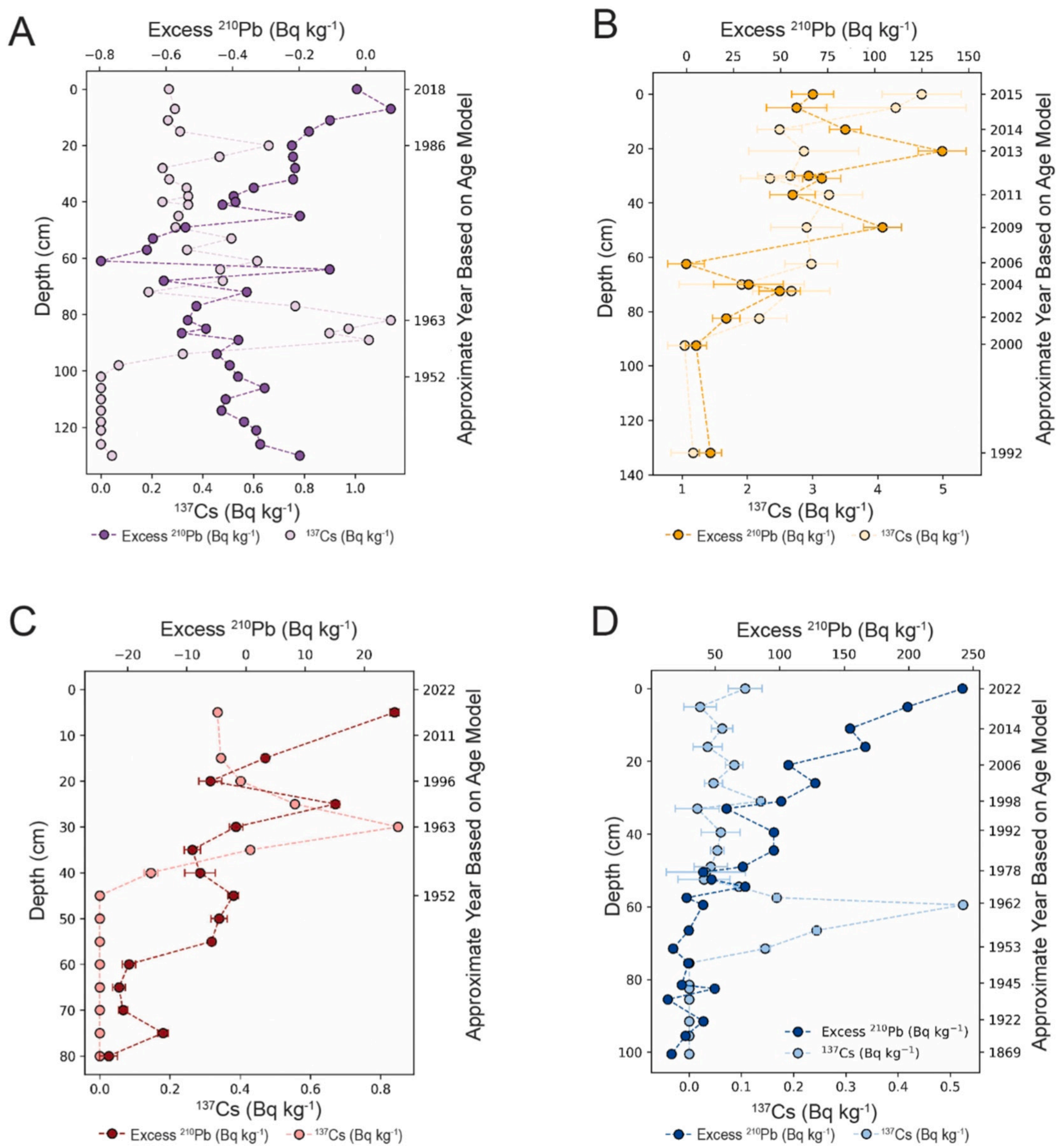

Fig. 3. The estimated age was based on the concentration of ^{210}Pb and ^{137}Cs along the depth of the sediment cores in Kiskiminetas River (A), Blacklick Creek (B), Raystown Lake (C), and Darby Creek (D). Sediment collected at the 135 cm depth in Blacklick Creek is estimated to date to 1992, while sediment cores from Kiskiminetas River (134 cm long), Raystown Lake (80 cm long), and Darby Creek (101 cm long) contained older sediments, predating 1950.

revealed a peak of ^{137}Cs at a depth of 60 cm and the presence of ^{137}Cs to a depth of approximately 75 cm. Excess ^{210}Pb concentration was detected slightly deeper in the sediment layers, allowing an *estimated* depositional age of the late 1800s at 100 cm depth (Fig. 3D).

Because the sedimentation rate can vary over time and radioactive age analysis differed among five locations, we calculated the sedimentation rate (cm yr^{-1}) based on the depth at which the presence of ^{137}Cs activity was first detected in the sediment core. Blacklick Creek showed

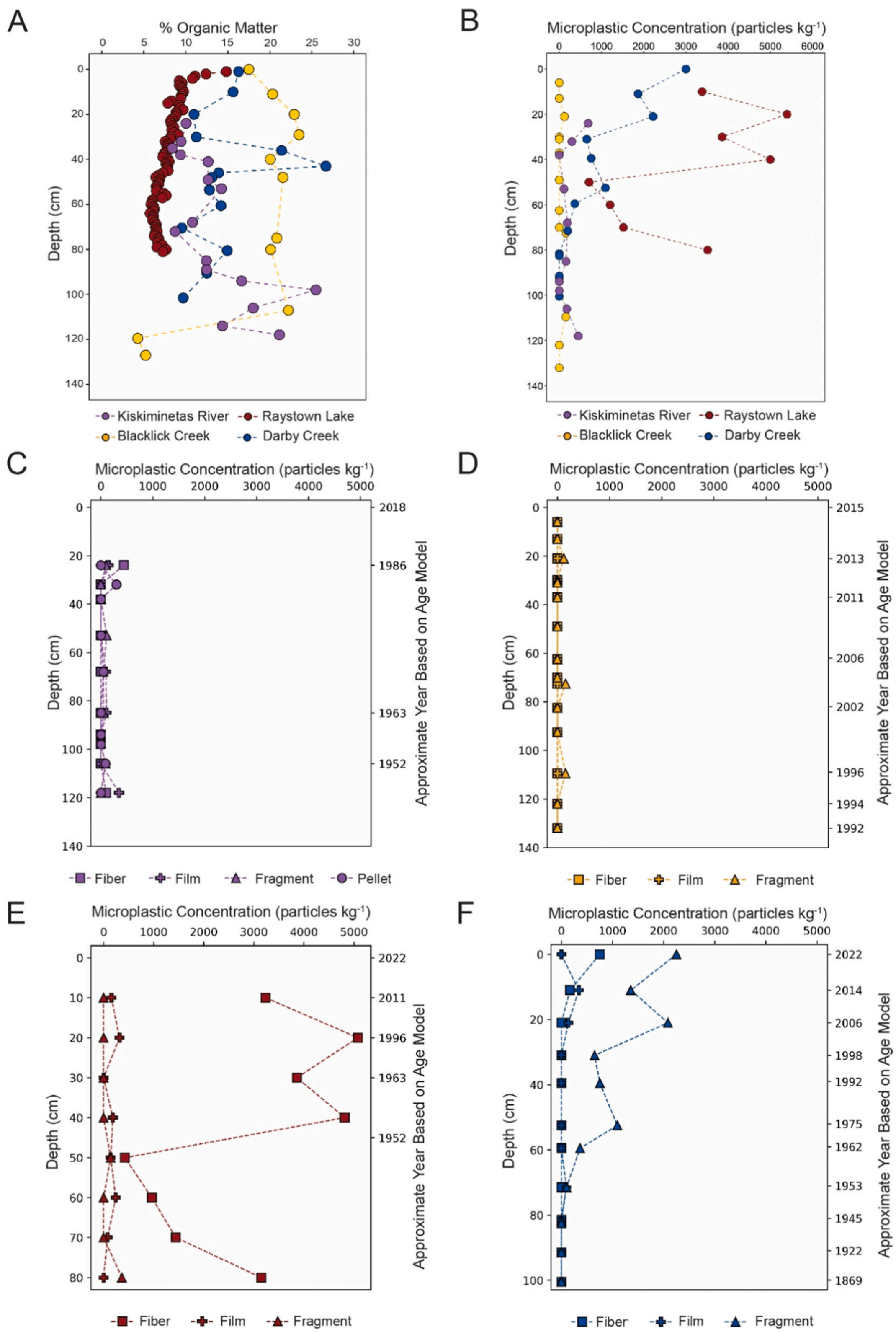

Fig. 4. Percentage of organic matter (A) and Microplastic concentration (B) versus depth in Kiskiminetas River (purple circle), Blacklick Creek (yellow circle), Raystown Lake (red circle), and Darby Creek (blue circle) cores. Microplastic abundance, categorized by microplastic morphology including fibers, films, fragments, and pellets versus depth and estimated age of sediment cores in Kiskiminetas River (C), Blacklick Creek (D), Raystown Lake (E), and Darby Creek (F).

^{137}Cs activity through the entire depth of the sediment core – so the entire 130 cm core (estimated age 1992) was used. The sedimentation rates were highest in Blacklick Creek at 5.74 cm $year^{-1}$, followed by Kiskiminetas River at 1.55 cm $year^{-1}$, Darby Creek at 1.04 cm $year^{-1}$, and Raystown Lake at 0.75 cm $year^{-1}$. We also calculated sedimentation rates for two cores with MP concentration profiles in other regions of the USA, Lake Mead at 1.83 cm $year^{-1}$ and Little Lake at 0.87 cm $year^{-1}$.

3.3. Organic matter

The average organic matter content varied between each core and with depth (Fig. 4A). Blacklick Creek contained the highest average organic matter content with 18 % compared to Kiskiminetas River (14.8 %), Raystown Lake (7.8 %), and Darby Creek (14.5 %). In the Kiskiminetas River, the organic matter profile showed an increasing trend with depth. Conversely, a decreasing organic matter profile with depth was observed in Raystown Lake. However, the organic matter content in Darby Creek spiked to 28 % at a depth of 40 cm and decreased to 15 % in the deeper sediment. Blacklick Creek showed an increasing organic matter content from 0 to 30 cm then consistent content (20–25 %) to 115 cm before a steep drop at the bottom of the core (>120 cm). We note that Blacklick Creek organic matter may be influenced by the presence of coal fines that resulted from coal mining in the region.

3.4. Microplastic concentrations and characteristics

All four locations contained detectable MP concentrations, but the depth profiles varied between sites (Fig. 4B). Blacklick Creek had the lowest MP concentrations among the locations, ranging between 0 (non-detect) to 156 particles kg^{-1} with very few detections overall. Similarly, the Kiskiminetas River was observed to have low MP concentrations, ranging from 0 to 448 particles kg^{-1}. In contrast, Raystown Lake sediment samples all contained MPs and exhibited a wide range of concentrations, varying from 704 to 5397 particles kg^{-1} with higher MP concentrations in the more recent sediment compared to deeper (older) portions of the core. Darby Creek MP concentrations ranged from 0 to 3000 particles kg^{-1} with a notable decrease in total MP with depth (age).

The dominant MP morphology also varied among the three sites (Fig. 4 C—F). MP fragments were dominant in Blacklick Creek and Darby Creek, while MP fibers were mainly found in Raystown Lake, and MP films were predominant in the Kiskiminestas River. Although variations of MP morphology and concentrations differed among the locations, they showed a similarity in color distribution (Fig. 5). Clear and blue MPs were the dominant colors where clear/blue MPs accounted for 65 %/17 % in Kiskiminetas River, 41 %/41 % in Blacklick Creek, 63 %/26 % in Raystown Lake, and 38 %/38 % in Darby Creek. While there were no distinguishable trends in MP size with depth in either Darby Creek or Raystown Lake (Fig. S3–A and S3—B), there was a significant difference (p-value = 0.0038) in fiber size between Raystown Lake and Darby Creek, particularly at the top of the sediment core (<40 cm) (Fig. S3—C). Fibers in Darby Creek were longer compared to those in Raystown Lake, while no significant difference was shown at the bottom of the sediment core (> 40 cm).

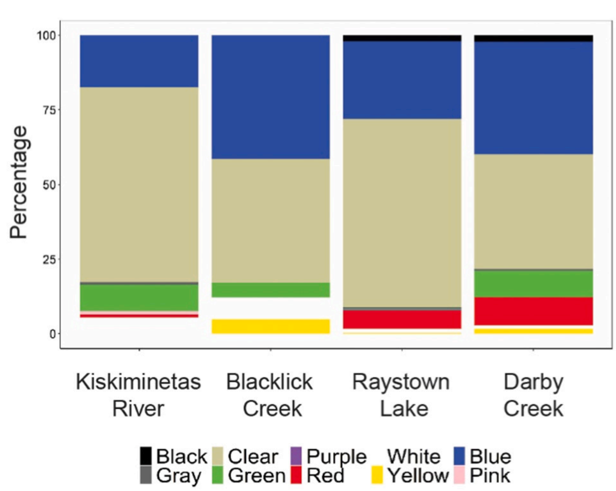

Fig. 5. The proportion of microplastic color in sediment cores collected in four sediment cores: Kiskiminetas River, Blacklick Creek, Raystown Lake, and Darby Creek.

3.5. Correlation analysis

The relationship between sedimentation rate and MP concentration was investigated in sediment cores in the four locations sampled in this study (Kiskiminetas River, Blacklick Creek, Raystown Lake, Darby Creek) as well as data obtained from two published studies, Little Lake and Lake Mead (Baldwin et al., 2020; Culligan et al., 2021). The average MP concentration at each location was calculated as a weighted average of the concentrations measured downcore to the depth where ^{137}Cs began to be detected. The MP concentration was weighted based on the depth between MP measurements, calculated as the ratio of total MP concentration to the depth of the sediment layer. The result showed a negative Pearson correlation between the log of depth-weighted average MP concentration and the log of sedimentation rate ($r = -0.82$, $p < 0.05$), as shown in (Fig. S7–A).

We also identified a negative Spearman relationship ($\rho = -0.42$) between the percent organic matter and the MP concentration at each sample depth with a p-value <0.05 ($n = 35$) (Fig. S7—B). The Raystown Lake core contained the lowest organic matter but the highest MP concentration. Likewise, the Blacklick Creek core contained high organic matter and lower MP concentrations, whereas Darby Creek was intermediate between Raystown Lake and Blacklick Creek for both organic content and MP concentration.

4. Discussion

4.1. Temporal distribution of microplastics

Based on the rapid increase of MP production from the 1950s to the present, we expected a similar increase in MP concentrations in the sediments deposited more recently and much lower MP concentrations in sediments at depth deposited before 1950. Despite a difference in average MP abundance between watersheds, we observed greater abundance in recent sediment in three of the four cores measured (Fig. 4). The exception is the Raystown Lake core, which had the highest overall MP detected as well as elevated concentrations of MP in sediment deposited prior to 1952. When averaged by decade across all four cores, we observe increased MPs (particle kg^{-1} $year^{-1}$) in more recent sediment (Fig. 6A, Table 2). The increase is statistically significant ($R^2 =$ 0.85 and p-value = 0.003) and corresponds to an increase in global plastic production (Fig. 6B). The estimated linear increase is roughly 32 MP counts per year per kilogram from 1950 to 2010. In comparison, Li et al. (2022) developed trend lines we estimated (visually) to increase between 0 and 14 MP counts per year per kilogram and an average increase closer to 3.3 in a subtropical lake setting over 1957–2018. Combined, our data demonstrate that freshwater sediments act as a sink for MPs and long-term sediment records track increases in MP accumulation over time that correspond to increased global plastic production. This type of information is not captured by modern surficial sediment or water sampling alone.

Interestingly, we observed a slight decrease in MPs (particle kg^{-1} $year^{-1}$) in the 2010–2020 data. While we consider this a preliminary finding, Baldwin et al. (2020) observed a similar pattern in MP counts of Lake Mead with lower values in 2010–present and higher counts in 2000–2010. While plastic production continued to increase from 2000

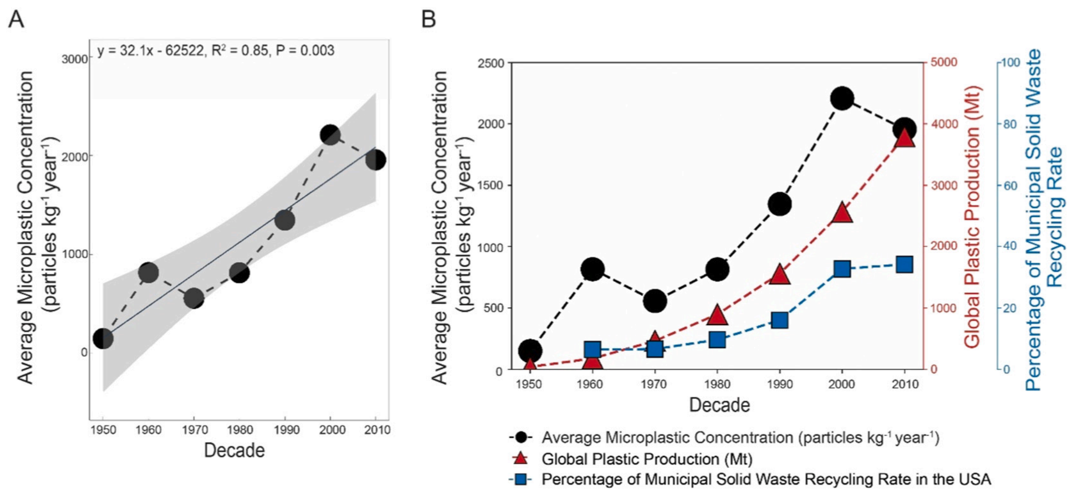

Fig. 6. The average MP contamination (particles kg^{-1} $year^{-1}$) from four sediment cores –Kiskiminetas River, Blacklick Creek, Raystown Lake (excluding 1950), and Darby Creek–from the 1950s to 2010s (A). The solid black line represents the regression line with a 95 % confidence interval (gray area). The increased trend of MPs in sediment showed a similar trend to the global plastic production in million metric tons (Mt), represented by the red triangle (B). In the 1960s, municipal solid waste recycling began in the USA and the recycling rate percentage (blue squares) increased, showing a slower increase in MP contamination in the sediment after the 1960s (Geyer et al., 2017; EPA, 2020).

Table 2
Average MP concentrations detected per decade from 1951 to 2022 in Kiskiminetas River, Blacklick Creek, Raystown Lake, and Darby Creek.

Year	Kiskiminetas River (particle kg^{-1} $year^{-1}$)	Blacklick Creek (particle kg^{-1} $year^{-1}$)	Raystown Lake (particle kg^{-1} $year^{-1}$)	Darby Creek (particle kg^{-1} $year^{-1}$)	Average combined (particle kg^{-1} $year^{-1}$)
2011–2022	nd	246	2821	2803	1957
2001–2010	nd	31	4048	2547	2209
1991–2000	nd	99	3238	702	1346
1981–1990	167	nd	1349	925	814
1971–1980	43	nd	1079	547	556
1961–1970	107	nd	2159	183	816
1951–1960	14	nd	6690	283	2329

Note: nd indicated no data available to perform MP analysis.

to 2020, there was also a rapid increase in recycling of plastic from 2000 onward, which may have reduced MPs that are improperly disposed of and accumulated as MPs in sediment (EPA, 2020; Geyer et al., 2017). This pattern is most evident in the Darby Creek core, located in a tidal estuary and one of the last sediment deposition areas before MP is transported to the ocean. Further sampling could focus on estuary environments and help quantify if this apparent reduction in MP accumulated in sediment is observed in other locations.

While Raystown Lake showed similar high concentrations in surface sediments that gradually decreased with depth, MP concentrations were high in sediment layers we interpreted as deposited before 1950. This similar, but surprising, abundance of MPs in the deeper sediments was also observed in a previous study of MPs in Lake Mead (Baldwin et al., 2020). The MPs in the Lake Mead study showed a similar morphology (99 % fibers) and color (clear 77.3 % and 10.2 % in blue) (Baldwin et al., 2020) to the Raytown Lake sediment core in our study.

Previous studies also reported inconsistent patterns in MP concentration and sediment age (Table 3). A decrease in MP abundance with increased sediment depth and age was reported at two sites in China, where MP abundance ranged between 0 and 1049 particles kg^{-1} and 107 to 1007 particles kg^{-1} in the Fuhe River and Xinghu Lake, respectively (Zhou et al., 2021, B. Li et al., 2022). Another study observed these trends in the Red River Delta and Tien Yen Bay in Northern Vietnam, where MP abundance ranged between 0 and 4941 particles kg^{-1} (Viet Dung et al., 2021). Similarly, the Roter Main River in southeast Germany showed a decreasing trend in MP abundance ranging from 4500 to 30,000 particles kg^{-1} (Frei et al., 2019).

In contrast, two studies have reported the highest MP abundance at depth, such as in cores collected from Lake Mead, Nevada, USA, where MP abundance ranged between 220 and 2040 particles kg^{-1} (Baldwin et al., 2020). In the Qinhuai River, China, MP abundance ranged between 163 and 563 particles kg^{-1} (Niu et al., 2021) with the highest concentrations observed in deeper intervals. MP abundance was also observed in cores collected from the Golden Horn Estuary in the Sea of Marmara, Turkey, with MPs ranging between 733 and 3000 particles kg^{-1}; however, the study did not observe changes in the depth or age of the sediment (Belivermiş et al., 2021).

As of 2022, only 20 studies focused on MP stratigraphy (Yuan et al., 2023). Of the 20, only three were conducted in freshwater environments and used some form of radiometric dating. As a result, data remains limited for understanding the temporal distribution of MP in freshwater sediments. Previous researchers suggested that the vertical transport of MPs could be influenced by various factors, including the sedimentation rate (Belivermiş et al., 2021), hydrodynamic conditions (Culligan et al., 2021; Niu et al., 2021), organisms (Gebhardt and Forster, 2018), and biofouling such as biofilm formation (Pete et al., 2023). These factors could disturb sediment and mix MPs into deeper, older sediment layers in some environments. MP particles were observed in sediment dated before 1950 in Raystown Lake (no ^{137}Cs detected), before mass plastic production (Geyer et al., 2017; Newton, 2021). Previous research that studied bioturbation as a mechanism for MP transport noted that the presence of the lugworm *Arenicola marina* in marine sediment was found to cause bidirectional MP transport in a mesocosm experiment (Gebhardt and Forster, 2018).

We should note that core sampling methods may move MPs during sample collection; however, we have limited data on how these methods disturb MP concentration in sediment cores. In our study, three different MP sampling methods were used. We noted no apparent MPs with sediments deposited before 1950 where we sampled with a Russian-style peat corer (Darby Creek and Kiskiminetas River), but elevated MPs in "old" sediment sampled with a percussion corer (Raystown Lake). In Lake Mead, which has a very similar MP profile to Raystown Lake core and Qinhuai River, we note that gravity coring was used with increased trends of MPs with depths (Baldwin et al., 2020; Niu et al., 2021). Other sample methods did not show any increased trends (Culligan et al., 2021; Niu et al., 2021). The gravity/piston sampling method may force

Table 3
Example studies of microplastic profiles in sediment cores.

Location	Country	Water type	Depth of sediment core (cm)	Range of MP concentration (particle kg^{-1})	MP profile trend with sediment depth	Radio-metric dating	Age	Core sampling method	Sampling date	Ref.
Red River Delta	Vietnam	Estuary	100	0–4941	Decreased trend	^{210}Pb	1937–2020	Peat sampler	2020	(Viet Dung et al., 2021)
Tien Yen Bay				0–815			1898–2020			
Jakarta	Indonesia	Estuary	88	69.86 ± 27.53[m], 78.52 ± 29.48[u]	Decreased trend	^{210}Pb and ^{137}Cs	Pre 1928–2023	Stainless steel tubes	2023	(Cordova et al., 2023)
Surabaya				103.17 ± 30.80[m], 103.00 ± 30.38[u]			Pre 1938–2023			
Cilacap				10.51 ± 5.06[m], 9.62 ± 7.56[u]			Pre 1893–2023*			
Berau				19.69 ± 10.93[m], 16.78 ± 12.83[u]			Pre 1921–2023+			
Little Lake	USA	Estuary	90	0–4366	Decreased trend	^{14}C and ^{137}Cs	Pre 1954–2016	Aluminum push core	November 2016	(Culligan et al., 2021)
Beibu Gulf	China	Marine	60	33–1200	Decreased trend	^{210}Pb and ^{137}Cs	1897–2017	Stainless-steel static gravity corer	July, 2017	(Xue et al., 2020)
Fuhe River	China	River	50	0–1049	Decreased trend	–	–	Columnar sampler	Not reported	(Zhou et al., 2021)
Xinghu Lake	China	Lake	40	107–1007	Decreased trend	^{210}Pb and ^{137}Cs	1957–2021	Column sediment sampler	March 2021	(B. Li et al., 2022)
Roter Main River	Germany	River	60	4500–30,000	Decreased trend	–	–	Freeze core sampling	May 2016 and August 2017	(Frei et al., 2019)
Lake Mead	USA	Lake	33	220–2040	Increased trend	^{137}Cs	2000–2018	Gravity corer with polycarbonate barrel	March 2018	(Baldwin et al., 2020)
Qinhuai River	China	River	50	163–563	Increased trend	–	–	Pistons and gravity corers	April 2019	(Niu et al., 2021)
Golden Horn Estuary	Turkey	Estuary	105	733–3000	No trend	^{210}Pb and ^{137}Cs	1903–2012	Gravity corer	2012	(Belivermiş et al., 2021)

* No MPs observed before 1893.
\+ No MPs observed before 1921.
[m] Mangrove.
[u] Mudflat.

MPs present in shallow sediment to depth, which are then observed in the older/deeper sediment profile.

4.2. Influencing factors on microplastic distribution

Recent studies suggest that human activities within a watershed significantly influence MP contamination (Baldwin et al., 2020; Belivermiş et al., 2021; B. Li et al., 2022). Surprisingly, our results are inconsistent with those studies. The most developed watershed in terms of land cover and population density, Darby Creek, did not exhibit the highest MP concentration. Instead, sediment from Raystown Lake, which has a much less developed area and lower population density, contained the highest average MP concentration. Meanwhile, low MP concentrations were observed in the Kiskiminetas River and Blacklick Creek despite nearly identical land development and population density as Raystown Lake. Our results suggest that highly urbanized areas may not always be the major contributors to MP contamination in freshwater environments, but instead, other factors may influence MP deposition and retention in sediment. Our GLR model identified only one statistically significant explanatory value, distance to sewage outfall. This significance was only apparent when Darby Creek, with zero upstream sewage discharge locations, was excluded from the model. While Darby Creek was the most populated watershed, the lack of high MPs present in Darby Creek relative to Raystown Lake could be explained by the lack of a wastewater treatment discharge.

One watershed factor that could help explain the high MP concentration in Raystown Lake is the open water area. The Raystown Lake watershed contained a much greater percentage of open water (17 %) than the Kiskiminetas River, Blacklick Creek, and Darby Creek watersheds, which each had <2 %. Open water areas could influence MP concentrations in sediments if airborne MP is a potential source of MPs within the watershed. Indeed, Baldwin et al. (2020) reported that atmospheric MP deposition could be a contamination source in Lake Mead. Despite its location in a less developed area, Lake Mead is downwind from urbanized areas and contains a high concentration of MPs. Likewise, many studies reported that atmospheric transport may play an important role in MP contamination in much more remote areas than our study, such as the Tibetan Plateau (Zhang et al., 2019), Pyrenees Mountains (Allen et al., 2019), Mount Everest (Napper et al., 2020), and rural areas (Klein and Fischer, 2019).

Furthermore, the location from which sediment cores are collected also impacts the MP concentration. For example, the Darby Creek sediment core was taken from the marsh platform, which is not continuously flooded. Therefore, deposition in this environment only captures some of the microplastics. For future research, it would be beneficial to sample in an area of deposition within the creek bed itself for a more direct comparison to the other sites.

Additionally, our results showed negative correlations between MP and sedimentation rate as well as organic matter content. The high sedimentation load in a watershed could result in the dilution of MP abundance (Saarni et al., 2023), which would indicate MPs are not directly correlated with sediment load within the watersheds. Regarding the relationship between MP and organic matter content, a laboratory experiment by Ivanic et al. (2023) reported that MPs can interact with dissolved organic matter through hydrophobic interactions, subsequently increasing the hydrophilicity of MP particles. This interaction could potentially enhance the mobility of MPs in the water phase, increasing the preference of MPs to remain in the water rather than settle in the sediment. Unfortunately, limited data are available on organic matter content in stratified sediment and its relationship with MPs in published studies to investigate this hypothesis. We do not observe nor do we expect to observe, MP abundance within a core to correlate with OM or sedimentation rate. This is for two reasons, 1) sedimentation rate does not change markedly within the cores and 2) MP abundance in sediment increases with time. Here we demonstrate that changes with MP over time are the major variable to predict MP abundance. However, we show that OM and sedimentation rate could help explain that variation across and between watersheds.

4.3. Microplastics morphology

Dominant MP morphology varied across the four watersheds. Raystown Lake showed the highest microplastic contamination, specifically fibers, while fragments were the dominant morphological type observed in Blacklick Creek and Darby Creek. Films were found to dominate in the Kiskiminetas River. The difference in morphologies could be linked to varying land cover types and human activities in these four locations (Tunali et al., 2022). For example, Raystown Lake has several popular recreational activities, such as hiking, camping, boating, and fishing, all of which may cause fiber contamination from visitor recreational clothing and gear. Conversely, Darby Creek had more diversity of microplastic types compared to Blacklick Creek, and Raystown Lake. High population density in Darby Creek may contribute to the usage of a variety of plastic types leading to various MP morphologies observed in Darby Creek. These findings align with a previous study showing greater diversity of MP morphologies in metropolitan areas (Baldwin et al., 2020).

The dominant MP color in our cores was clear, which may result from widely used transparent plastic products, such as packaging bags or discoloration of colored plastic from environmental processes or our organic matter removal process (H_2O_2) during MP extraction in the lab (Baldwin et al., 2020; Drabinski et al., 2023; Matjašič et al., 2023; Munno et al., 2018). To avoid discoloration during the digestion process, it is important to take precautions to prevent overreaction and minimize heat generation due to exothermic reactions during the organic removal process (Munno et al., 2018). The source of blue coloration is less certain, but it is consistent with previously published studies (Baldwin et al., 2020; Yubo Li et al., 2020). Many studies reported that organisms exhibit color preferences in MP uptake, which impacts the concentration of MP exposure to organisms and the MPs found in the environment (Huang et al., 2021; Okamoto et al., 2022). It is possible that the predominant MP colors found in this study are related to the MP consumption by organisms. These organisms may mistakenly consume MPs with colors that are similar to natural materials in the local environment or their foods (Huang et al., 2021).

MP size was similar between watersheds and did not vary with depth. However, significantly longer fibers were observed in Darby Creek compared to Raystown Lake. The longer water residence time in the lake may contribute to a higher degree of weathering influenced by abiotic degradation (from sunlight, temperature, and mechanical stress) and biotic degradation, resulting in smaller MP (Kalogerakis et al., 2017; Loague and Corwin, 2007; Sutkar et al., 2023). The observation of shorter fibers in Raystown Lake might contribute to the greater abundance of MP in sediments. However, the overall mass of MPs in both locations may be similar but would require alternative measurements to quantify. MPs reported on a mass per mass basis may lead to different conclusions than a count per mass as reported here and in most other studies on MPs. In future studies, consistent MP units, extraction methods, and standardized guidelines are crucial for researchers to compare results, elaborate on research, and assess environmental impact accurately and reliably.

5. Conclusion

Our results revealed that MP deposition in freshwater sediments increased from 1950s to 2010s. This increase corresponded to the overall increase in plastics production during the same period. MP abundance varied widely between watersheds with generally higher concentrations observed in the most recent sediment but with some MPs observed in sediment older than ~1950s. While human activities within a watershed tend to promote a variety of MP morphologies, surprisingly, land use and population density within watersheds did not correlate to MP abundance in older sediment. Instead, the highest MP abundance was observed in a watershed with low urbanization, but a high percentage of open water, which could indicate a contribution from atmospheric MP deposition. Further exploration of these relationships is crucial to developing effective strategies for mitigating MP pollution in freshwater environments. Additionally, we calculated an average increase of ~33 MP counts/year/kg in sediment. The increase in MP in the freshwater aquatic environment corresponding to plastic production indicates that greater recycling and perhaps regulatory controls are necessary to reduce plastic flux to water systems.

CRediT authorship contribution statement

Jutamas Bussarakum: Writing – original draft, Visualization, Validation, Methodology, Investigation, Formal analysis, Data curation. **William D. Burgos:** Writing – review & editing, Methodology, Investigation, Funding acquisition. **Samuel B. Cohen:** Methodology, Investigation, Formal analysis. **Kimberly Van Meter:** Writing – review & editing, Methodology, Investigation, Funding acquisition, Conceptualization. **Jon N. Sweetman:** Writing – review & editing, Methodology, Investigation, Funding acquisition. **Patrick J. Drohan:** Writing – review & editing, Methodology, Investigation. **Raymond G. Najjar:** Writing – review & editing, Funding acquisition, Conceptualization. **Jill M. Arriola:** Writing – review & editing, Validation, Methodology, Investigation, Formal analysis, Data curation, Conceptualization. **Katharina Pankratz:** Methodology, Formal analysis. **Lisa A. Emili:** Writing – review & editing, Writing – original draft, Visualization, Validation, Supervision, Resources, Project administration, Methodology, Investigation, Funding acquisition, Formal analysis, Data curation, Conceptualization. **Nathaniel R. Warner:** Writing – review & editing, Visualization, Validation, Supervision, Resources, Project administration, Methodology, Investigation, Funding acquisition, Formal analysis, Data curation, Conceptualization.

Declaration of generative AI and AI-assisted technologies in the writing process

During the preparation of this work, author Bussarakum used ChatGPT in order to improve grammar and readability of early drafts. After using this tool/service, the author(s) reviewed and edited the content as needed and take(s) full responsibility for the content of the publication.

Declaration of competing interest

Nathaniel R. Warner reports financial support was provided by National Science Foundation. JB was supported by a Royal Thai Government Scholarship. If there are other authors, they declare that they have no known competing financial interests or personal relationships that could have appeared to influence the work reported in this paper.

Data availability

Data will be made available on request.

Acknowledgements

JB was supported by a Royal Thai Government Scholarship. We acknowledge that ChatGPT was used by JB for earlier drafts to help with the editing of English. Funding from NSF 1942601 helped support the analysis. Support was also provided by The Pennsylvania State University Commonwealth Campuses Center Nodes (C3N) and the Institute of Energy and the Environment Seed Grant programs.

We gratefully acknowledge the in-kind support and assistance with core collection at the Darby Creek site provided by J. Greg Taylor and Robert Tunstead, Soil and Plant Science Division, USDA-NRCS. We thank Lamar Gore, Mariana Bergerson, and Garrett White (U.S. Fish and Wildlife Service) for access to the John Heinz Wildlife Refuge at Tinicum and support with sample collection and logistics. We thank Carol Armstrong and Ann Faulds of the Friends of Heinz for their assistance with field site selection. We gratefully acknowledge assistance in the field provided by Daniel Guarin, Matthew James, and Dylan McClellan.

Thank you to Dr. Sharon Yohn and Chuck Yohn of the Juniata College Raystown Field Station for providing lodging, logistical support, and expert boat navigation crucial to the collection of the Raystown Lake sediment core. Thank you to Zachary Van Eyken and Alainna Nevling for their assistance in the collection, processing, and analysis of Raystown Lake sediment core samples.

Appendix A. Supplementary data

Supplementary data to this article can be found online at https://doi.org/10.1016/j.scitotenv.2024.176619.

References

Allegheny Ridge Corporation, 2023. Kiski-Conemaugh River Water Trail. https://mainlinecanalgreenway.org/wp-content/uploads/2023/12/KC-WT-Lower-FINAL_printer-friendly-maps.pdf.

Allen, S., Allen, D., Phoenix, V.R., Le Roux, G., Durántez Jiménez, P., Simonneau, A., Binet, S., Galop, D., 2019. Atmospheric transport and deposition of microplastics in a remote mountain catchment. Nat. Geosci. 12 (5), 339–344. https://doi.org/10.1038/s41561-019-0335-5.

Andrady, A.L., 2011. Microplastics in the marine environment. Mar. Pollut. Bull. 62 (8), 1596–1605. https://doi.org/10.1016/j.marpolbul.2011.05.030.

Baldwin, A.K., Spanjer, A.R., Rosen, M.R., Thom, T., 2020. Microplastics in Lake Mead National Recreation Area, USA: occurrence and biological uptake. PLoS One 15 (5). https://doi.org/10.1371/journal.pone.0228896.

Baud, A., Aulard, C., Ghanbari, H., Fradette, M., Antoniades, D., del Giorgio, P., Huot, Y., Francus, P., Smol, J., Gregory-Eaves, I., 2022. A framework for 210Pb model selection and its application to 37 cores from eastern Canada to identify the dynamics and drivers of lake sedimentation rates. Earth Surf. Process. Landf. 47 (10), 2518–2530. https://doi.org/10.1002/esp.5391.

Belivermiş, M., Kılıç, Ö., Sezer, N., Sıkdokur, E., Güngör, N.D., Altuğ, G., 2021. Microplastic inventory in sediment profile: A case study of Golden Horn Estuary, Sea of Marmara. Mar. Pollut. Bull. 173, 113117. https://doi.org/10.1016/j.marpolbul.2021.113117.

Ben-David, E.A., Habibi, M., Haddad, E., Hasanin, M., Angel, D.L., Booth, A.M., Sabbah, I., 2021. Microplastic distributions in a domestic wastewater treatment plant: removal efficiency, seasonal variation and influence of sampling technique. Sci. Total Environ. 752, 141880. https://doi.org/10.1016/j.scitotenv.2020.141880.

Burgos, W.D., Castillo-Meza, L., Tasker, T.L., Geeza, T.J., Drohan, P.J., Liu, X., Landis, J. D., Blotevogel, J., McLaughlin, M., Borch, T., Warner, N.R., 2017. Watershed-scale impacts from surface water disposal of oil and gas wastewater in Western Pennsylvania. Environ. Sci. Technol. 51 (15), 8851–8860. https://doi.org/10.1021/ACS.EST.7B01696/SUPPL_FILE/ES7B01696_SI_001.PDF.

Cordova, M.R., Ulumuddin, Y.I., Lubis, A.A., Kaisupy, M.T., Wibowo, S.P.A., Subandi, R., Yogaswara, D., Purbonegoro, T., Renyaan, J., Nurdiansah, D., Sugiharto, U., Shintianata, D., Meiliastri, S.S., Andini, F.P., Suratno, Ilman, Anggoro, M., Basir, A. W., Cragg, S.M., 2023. Microplastics leaving a trace in mangrove sediments ever since they were first manufactured: a study from Indonesia mangroves. Mar. Pollut. Bull. 195, 115517. https://doi.org/10.1016/j.marpolbul.2023.115517.

Culligan, N., Liu, K., Ribble, K., Ryu, J., Dietz, M., 2021. Sedimentary records of microplastic pollution from coastal Louisiana and their environmental implications. J. Coast. Conserv. 26 (1), 1. https://doi.org/10.1007/s11852-021-00847-y.

D'Avignon, G., Gregory-Eaves, I., Ricciardi, A., 2021. Microplastics in lakes and rivers: an issue of emerging significance to limnology. Environ. Rev. 30 (2), 228–244. https://doi.org/10.1139/er-2021-0048.

De Souza, V. L. B., Rodrigues, K. R. G., Pedroza, E. H., Melo, R. T. de, Lima, V. L. de, Hazin, C. A., Almeida, M. G. O. de, & Nascimento, R. K. do. (2012). Sedimentation Rate and 210Pb Sediment Dating at Apipucos Reservoir, Recife, Brazil. In Sustainability (Vol. 4, Issue 10, pp. 2419–2429). doi:https://doi.org/10.3390/su4102419.

De Witte, B., Devriese, L., Bekaert, K., Hoffman, S., Vandermeersch, G., Cooreman, K., Robbens, J., 2014. Quality assessment of the blue mussel (Mytilus edulis): comparison between commercial and wild types. Mar. Pollut. Bull. 85 (1), 146–155. https://doi.org/10.1016/j.marpolbul.2014.06.006.

Dong, M., Luo, Z., Jiang, Q., Xing, X., Zhang, Q., Sun, Y., 2020. The rapid increases in microplastics in urban lake sediments. Sci. Rep. 10 (1), 848. https://doi.org/10.1038/s41598-020-57933-8.

Drabinski, T.L., de Carvalho, D.G., Gaylarde, C.C., Lourenço, M.F.P., Machado, W.T.V., da Fonseca, E.M., da Silva, A.L., Baptista Neto, J.A., 2023. Microplastics in freshwater river in Rio de Janeiro and its role as a source of microplastic pollution in Guanabara Bay, SE Brazil. Micro 3 (1), 208–223. https://doi.org/10.3390/micro3010015.

Duong, T.T., Le, P.T., Nguyen, T.N.H., Hoang, T.Q., Ngo, H.M., Doan, T.O., Le, T.P.Q., Bui, H.T., Bui, M.H., Trinh, V.T., Nguyen, T.L., Da Le, N., Vu, T.M., Tran, T.K.C., Ho, T.C., Phuong, N.N., Strady, E., 2022. Selection of a density separation solution to study microplastics in tropical riverine sediment. Environ. Monit. Assess. 194 (2), 65. https://doi.org/10.1007/S10661-021-09664-0.

EPA, 2020. Advancing Sustainable Materials Management: 2018 Fact Sheet. https://www.epa.gov/sites/default/files/2021-01/documents/2018_ff_fact_sheet_dec_2020_fnl_508.pdf.

Europe, P., 2022. Plastics–the facts 2022. PlasticEurope 1, 1–81.

Felipe-Rodríguez, M., Böhm, G., Doran, R., 2022. What does the public think about microplastics? Insights from an empirical analysis of mental models elicited through free associations. Front. Psychol. 13. https://doi.org/10.3389/fpsyg.2022.920454.

Free, C.M., Jensen, O.P., Mason, S.A., Eriksen, M., Williamson, N.J., Boldgiv, B., 2014. High-levels of microplastic pollution in a large, remote, mountain lake. Mar. Pollut. Bull. 85 (1), 156–163. https://doi.org/10.1016/j.marpolbul.2014.06.001.

Frei, S., Piehl, S., Gilfedder, B.S., Löder, M.G.J., Krutzke, J., Wilhelm, L., Laforsch, C., 2019. Occurence of microplastics in the hyporheic zone of rivers. Sci. Rep. 9 (1), 15256. https://doi.org/10.1038/s41598-019-51741-5.

Frias, J.P.G.L., Nash, R., 2019. Microplastics: finding a consensus on the definition. Mar. Pollut. Bull. 138, 145–147. https://doi.org/10.1016/j.marpolbul.2018.11.022.

Frias, J., Pagter, E., Nash, R., O'Connor, I., Carretero, O., Filgueiras, A., Viñas, L., Gago, J., Antunes, J., Bessa, F., Sobral, P., Goruppi, A., Tirelli, V., Pedrotti, M.L., Suaria, G., Aliani, S., Lopes, C., Raimundo, J., Caetano, M., Gerdts, G., 2018. Standardised protocol for monitoring microplastics in sediments. https://doi.org/10.13140/RG.2.2.36256.89601/1.

Gebhardt, C., Forster, S., 2018. Size-selective feeding of Arenicola marina promotes long-term burial of microplastic particles in marine sediments. Environ. Pollut. (Barking, Essex : 1987) 242 (Pt B), 1777–1786. https://doi.org/10.1016/j.envpol.2018.07.090.

Geyer, R., Jambeck, J.R., Law, K.L., 2017. Production, use, and fate of all plastics ever made. Sci. Adv. 3 (7), 1700782. https://doi.org/10.1126/SCIADV.1700782.

Glew, J.R., Smol, J.P., Last, W.M., 2001. In: Last, W.M., Smol, J.P. (Eds.), Sediment Core Collection and Extrusion BT - Tracking Environmental Change Using Lake Sediments: Basin Analysis, Coring, and Chronological Techniques. Springer, Netherlands, pp. 73–105. https://doi.org/10.1007/0-306-47669-X_5.

Hanif, M.A., Ibrahim, N., Dahalan, F.A., Md Ali, U.F., Hasan, M., Jalil, A.A., 2022. Microplastics and nanoplastics: recent literature studies and patents on their removal from aqueous environment. Sci. Total Environ. 810, 152115. https://doi.org/10.1016/j.scitotenv.2021.152115.

Heiri, O., Lotter, A.F., Lemcke, G., 2001. Loss on ignition as a method for estimating organic and carbonate content in sediments: reproducibility and comparability of results. J. Paleolimnol. 25 (1), 101–110. https://doi.org/10.1023/A:1008119611481.

Huang, Y., Xiao, X., Effiong, K., Xu, C., Su, Z., Hu, J., Jiao, S., Holmer, M., 2021. New insights into the microplastic enrichment in the blue carbon ecosystem: evidence from seagrass meadows and mangrove forests in coastal South China Sea. Environ. Sci. Technol. 55 (8), 4804–4812. https://doi.org/10.1021/acs.est.0c07289.

Ivanic, F.M., Guggenberger, G., Woche, S.K., Bachmann, J., Hoppe, M., Carstens, J.F., 2023. Soil organic matter facilitates the transport of microplastic by reducing surface hydrophobicity. Colloids Surf. A Physicochem. Eng. Asp. 676, 132255. https://doi.org/10.1016/j.colsurfa.2023.132255.

Jambeck, J.R., Walker-Franklin, I., 2023. The impacts of plastics' life cycle. One Earth 6 (6), 600–606. https://doi.org/10.1016/j.oneear.2023.05.015.

Jiang, Y., Xia, W., Zhao, R., Wang, M., Tang, J., Wei, Y., 2021. Insight into the interaction between microplastics and microorganisms based on a bibliometric and visualized analysis. Bull. Environ. Contam. Toxicol. 107 (4), 585–596. https://doi.org/10.1007/S00128-021-03201-Y/FIGURES/6.

Kalogerakis, N., Karkanorachaki, K., Kalogerakis, G.C., Triantafyllidi, E.I., Gotsis, A.D., Partsinevelos, P., Fava, F., 2017. Microplastics generation: onset of fragmentation of polyethylene films in marine environment Mesocosms. Front. Mar. Sci. 4. https://www.frontiersin.org/articles/10.3389/fmars.2017.00084.

Kannan, K., Vimalkumar, K., 2021. A review of human exposure to microplastics and insights into microplastics as obesogens. Front. Endocrinol. 12 (August), 1–19. https://doi.org/10.3389/fendo.2021.724989.

Kazmiruk, T.N., Kazmiruk, V.D., Bendell, L.I., 2018. Abundance and distribution of microplastics within surface sediments of a key shellfish growing region of Canada. PLoS One 13 (5), e0196005. https://doi.org/10.1371/journal.pone.0196005.

Klein, M., Fischer, E.K., 2019. Microplastic abundance in atmospheric deposition within the metropolitan area of Hamburg, Germany. Sci. Total Environ. 685, 96–103. https://doi.org/10.1016/j.scitotenv.2019.05.405.

Koutnik, V.S., Leonard, J., Alkidim, S., DePrima, F.J., Ravi, S., Hoek, E.M.V., Mohanty, S. K., 2021. Distribution of microplastics in soil and freshwater environments: global

analysis and framework for transport modeling. Environ. Pollut. 274, 116552. https://doi.org/10.1016/j.envpol.2021.116552.
Leslie, H.A., van Velzen, M.J.M., Brandsma, S.H., Vethaak, A.D., Garcia-Vallejo, J.J., Lamoree, M.H., 2022. Discovery and quantification of plastic particle pollution in human blood. Environ. Int. 163, 107199. https://doi.org/10.1016/j.envint.2022.107199.
Li, Yubo, Lu, Z., Zheng, H., Wang, J., Chen, C., 2020. Microplastics in surface water and sediments of Chongming Island in the Yangtze estuary, China. Environ. Sci. Eur. 32 (1), 15. https://doi.org/10.1186/s12302-020-0297-7.
Li, B., Wan, H., Cai, Y.P., Peng, J.P., Li, B.W., Jia, Q.P., Yuan, X., Wang, Y.Y., Zhang, P., Hong, B., Yang, Z.F., 2022. Human activities affect the multidecadal microplastic deposition records in a subtropical urban lake, China. Sci. Total Environ. 820. https://doi.org/10.1016/j.scitotenv.2022.153187.
Li, Yue, Tao, L., Wang, Q., Wang, F., Li, G., Song, M., 2023. Potential health impact of microplastics: A review of environmental distribution, human exposure, and toxic effects. Environ. Health 1 (4), 249–257. https://doi.org/10.1021/envhealth.3c00052.
Lin, Z., Jin, T., Zou, T., Xu, L., Xi, B., Xu, D., He, J., Xiong, L., Tang, C., Peng, J., Zhou, Y., Fei, J., 2022. Current progress on plastic/microplastic degradation: fact influences and mechanism. Environ. Pollut. 304, 119159. https://doi.org/10.1016/j.envpol.2022.119159.
Loague, K., Corwin, D., 2007. Scale Issues, pp. 25.1–25.21.
Ma, L., Wu, J., Abuduwaili, J., 2013. Climate and environmental changes over the past 150 years inferred from the sediments of Chaiwopu Lake, central Tianshan Mountains, Northwest China. Int. J. Earth Sci. 102 (3), 959–967. https://doi.org/10.1007/s00531-012-0838-4.
Matjašič, T., Mori, N., Hostnik, I., Bajt, O., Kovač Viršek, M., 2023. Microplastic pollution in small rivers along rural–urban gradients: variations across catchments and between water column and sediments. Sci. Total Environ. 858, 160043. https://doi.org/10.1016/j.scitotenv.2022.160043.
Mendrik, F., Fernández, R., Hackney, C.R., Waller, C., Parsons, D.R., 2023. Non-buoyant microplastic settling velocity varies with biofilm growth and ambient water salinity. Comm. Earth Environ. 4 (1), 30. https://doi.org/10.1038/s43247-023-00690-z.
Moyal, J., Dave, P.H., Wu, M., Karimpour, S., Brar, S.K., Zhong, H., Kwong, R.W.M., 2023. Impacts of biofilm formation on the physicochemical properties and toxicity of microplastics: A concise review. Rev. Environ. Contam. Toxicol. 261 (1), 8. https://doi.org/10.1007/s44169-023-00035-z.
Munno, K., Helm, P.A., Jackson, D.A., Rochman, C., Sims, A., 2018. Impacts of temperature and selected chemical digestion methods on microplastic particles. Environ. Toxicol. Chem. 37 (1), 91–98. https://doi.org/10.1002/etc.3935.
Napper, I.E., Davies, B.F.R., Clifford, H., Elvin, S., Koldewey, H.J., Mayewski, P.A., Miner, K.R., Potocki, M., Elmore, A.C., Gajurel, A.P., Thompson, R.C., 2020. Reaching New Heights in plastic pollution—preliminary findings of microplastics on Mount Everest. One Earth 3 (5), 621–630. https://doi.org/10.1016/j.oneear.2020.10.020.
Newton, D.E., 2021. Plastics and Microplastics: A Reference Handbook. Bloomsbury Publishing USA.
Niu, L., Li, Y., Li, Y., Hu, Q., Wang, C., Hu, J., Zhang, W., Wang, L., Zhang, C., Zhang, H., 2021. New insights into the vertical distribution and microbial degradation of microplastics in urban river sediments. Water Res. 188, 116449. https://doi.org/10.1016/j.watres.2020.116449.
Okamoto, K., Nomura, M., Horie, Y., Okamura, H., 2022. Color preferences and gastrointestinal-tract retention times of microplastics by freshwater and marine fishes. Environ. Pollut. 304, 119253. https://doi.org/10.1016/j.envpol.2022.119253.
Osorio, E.D., Tanchuling, M.A.N., Diola, M.B.L.D., 2021. Microplastics occurrence in surface waters and sediments in five river mouths of Manila Bay. Front. Environ. Sci. 9. https://www.frontiersin.org/articles/10.3389/fenvs.2021.719274.
Peng, L., Fu, D., Qi, H., Lan, C.Q., Yu, H., Ge, C., 2020. Micro- and nano-plastics in marine environment: source, distribution and threats — A review. Sci. Total Environ. 698, 134254. https://doi.org/10.1016/j.scitotenv.2019.134254.
Pennsylvania Department of Environmental Protection, 2023a. NPDES Permit Fact Sheet: Individual Sewage. https://files.dep.state.pa.us/water/wastewatermanagement/EDMRPortalFiles/Permits/PA0084883_FACT_SHEET_20230418_DRAFT_V3.pdf.
Pennsylvania Department of Environmental Protection, 2023b. Water pollution control facilities [data set]. https://www.pasda.psu.edu/uci/DataSummary.aspx?dataset=288.
Pennsylvania Department of Environmental Protection, 2023c. Water resources [data set]. https://www.pasda.psu.edu/uci/DataSummary.aspx?dataset=289.
Pete, A.J., Brahana, P.J., Bello, M., Benton, M.G., Bharti, B., 2023. Biofilm formation influences the wettability and settling of microplastics. Environ. Sci. Technol. Lett. 10 (2), 159–164. https://doi.org/10.1021/acs.estlett.2c00728.
Rogers, K.L., Carreres-Calabuig, J.A., Gorokhova, E., Posth, N.R., 2020. Micro-by-micro interactions: how microorganisms influence the fate of marine microplastics. Limnol. Oceanograph. Lett. 5 (1), 18–36. https://doi.org/10.1002/lol2.10136.
Saarni, S., Soininen, T., Uurasjärvi, E., Hartikainen, S., Meronen, S., Saarinen, T., Koistinen, A., 2023. Seasonal variation observed in microplastic deposition rates in boreal lake sediments. J. Soils Sediments 23 (4), 1960–1970. https://doi.org/10.1007/s11368-023-03465-3.
Sanchez-Cabeza, J.A., Ruiz-Fernández, A.C., 2012. 210Pb sediment radiochronology: an integrated formulation and classification of dating models. Geochim. Cosmochim. Acta 82, 183–200. https://doi.org/10.1016/j.gca.2010.12.024.
Senathirajah, K., Attwood, S., Bhagwat, G., Carbery, M., Wilson, S., Palanisami, T., 2021. Estimation of the mass of microplastics ingested – A pivotal first step towards human health risk assessment. J. Hazard. Mater. 404, 124004. https://doi.org/10.1016/j.jhazmat.2020.124004.
Skilbeck, C., Trevathan-Tackett, S., Apichanangkool, P., Macreadie, P., 2017. Sediment sampling in estuaries: site selection and sampling. Techniques 20, 89–120. https://doi.org/10.1007/978-94-024-0990-1_5.
Smol, J.P., 2019. Under the radar: long-term perspectives on ecological changes in lakes. Proc. R. Soc. B Biol. Sci. 286 (1906), 20190834. https://doi.org/10.1098/rspb.2019.0834.
Sutkar, P.R., Gadewar, R.D., Dhulap, V.P., 2023. Recent trends in degradation of microplastics in the environment: A state-of-the-art review. J. Hazard. Mater. Adv. 11, 100343. https://doi.org/10.1016/j.hazadv.2023.100343.
Tunali, M.M., Myronyuk, O., Tunali, M., Yenigün, O., 2022. Microplastic abundance in human-influenced soils in recreational, residential, and industrial areas. Water Air Soil Pollut. 233 (11), 433. https://doi.org/10.1007/s11270-022-05901-5.
Turner, S., Horton, A.A., Rose, N.L., Hall, C., 2019. A temporal sediment record of microplastics in an urban lake, London, UK. J. Paleolimnol. 61 (4), 449–462. https://doi.org/10.1007/s10933-019-00071-7.
Viet Dung, L., Huu Duc, T., Thi Khanh Linh, L., Thi Dieu Ly, T., Anh Duong, H., Thi My Hao, N., 2021. Depth profiles of microplastics in sediment cores from two mangrove forests in northern Vietnam. J. Marine Sci. Eng. 9, Issue 12. https://doi.org/10.3390/jmse9121381.
Villanova-Solano, C., Hernández-Sánchez, C., Díaz-Peña, F.J., González-Sálamo, J., González-Pleiter, M., Hernández-Borges, J., 2023. Microplastics in snow of a high mountain national park: El Teide, Tenerife (Canary Islands, Spain). Sci. Total Environ. 873, 162276. https://doi.org/10.1016/j.scitotenv.2023.162276.
Walker, T.R., 2021. (Micro)plastics and the UN sustainable development goals. Curr. Opinion Green Sustain. Chem. 30, 100497. https://doi.org/10.1016/j.cogsc.2021.100497.
Wang, J., Baskaran, M., Cukrov, N., Du, J., 2022. Geochemical mobility of 137Cs in marine environments based on laboratory and field studies. Chem. Geol. 614, 121179. https://doi.org/10.1016/j.chemgeo.2022.121179.
Wickham, J., Stehman, S.V., Sorenson, D.G., Gass, L., Dewitz, J.A., 2021. Thematic accuracy assessment of the NLCD 2016 land cover for the conterminous United States. Remote Sens. Environ. 257, 112357. https://doi.org/10.1016/j.rse.2021.112357.
Xue, B., Zhang, L., Li, R., Wang, Y., Guo, J., Yu, K., Wang, S., 2020. Underestimated microplastic pollution derived from fishery activities and "hidden" in deep sediment. Environ. Sci. Technol. 54 (4), 2210–2217. https://doi.org/10.1021/acs.est.9b04850.
Yuan, B., Gan, W., Sun, J., Lin, B., Chen, Z., 2023. Depth profiles of microplastics in sediments from inland water to coast and their influential factors. Sci. Total Environ. 903, 166151. https://doi.org/10.1016/j.scitotenv.2023.166151.
Zhang, Y., Gao, T., Kang, S., Sillanpää, M., 2019. Importance of atmospheric transport for microplastics deposited in remote areas. Environ. Pollut. 254, 112953. https://doi.org/10.1016/j.envpol.2019.07.121.
Zhou, Z., Zhang, P., Zhang, G., Wang, S., Cai, Y., Wang, H., 2021. Vertical microplastic distribution in sediments of Fuhe River estuary to Baiyangdian wetland in northern China. Chemosphere 280, 130800. https://doi.org/10.1016/j.chemosphere.2021.130800.
Zhu, Xia, 2021. The plastic cycle – an unknown branch of the carbon cycle. Front. Mar. Sci. 7. https://doi.org/10.3389/fmars.2020.609243.
Zhu, Xiaopeng, Ran, W., Teng, J., Zhang, C., Zhang, W., Hou, C., Zhao, J., Qi, X., Wang, Q., 2021. Microplastic pollution in nearshore sediment from the Bohai Sea coastline. Bull. Environ. Contam. Toxicol. 107 (4), 665–670. https://doi.org/10.1007/s00128-020-02866-1.